Transactions

RRFM 2010

Marrakech, Morocco
21 -25 March 2010

organised in cooperation with:

IAEA
International Atomic Energy Agency
Atoms For Peace

European Nuclear Society
Rue Belliard 65
1040 Brussels, Belgium
Phone + 32 2 505 30 54
Fax +32 2 502 39 02
E-mail ens@euronuclear.org
Internet www.euronuclear.org

ISBN 978-92-95064-10-2

These transactions contain all contributions submitted by 19 March 2010.

TRIGA Session:

Application of RELAP/SCDAPSIM to TRIGA System Thermal Hydraulic Analysis

C. M. ALLISON, J. K. HOHORST
Innovative Systems Software, LLC
Idaho Falls, Idaho 83404 USA
iss@relap.com

Md.Quamrul Huda
Atomic Energy Research Establishment
GPO Box 3787, Dhaka-1000
Bangladesch
quamrul@dhaka.net

ABSTRACT

The RELAP/SCDAPSIM/MOD4.0 code, designed to predict the behavior of reactor systems during normal and accident conditions, is being developed as part of the international SCDAP Development and Training Program (SDTP). RELAP/SCDAPSIM/MOD4.0, which is the first version of RELAP5 completely rewritten to FORTRAN 90/95/2000 standards, uses publicly available RELAP5 and SCDAP models in combination with advanced programming and numerical techniques and other SDTP-member modeling/user options. This paper describes the development of a representative input model for the 3MW TRIGA research reactor at AERE Bangladesh, describes the testing and qualification of the model using MOD4.0 advanced input checking and graphical display options, and then presents representative results for selected calculations.

1. Introduction

RELAP/SCDAPSIM[1-4], designed to predict the behavior of reactor systems during normal and accident conditions, is being developed at Innovative Systems Software (ISS) as part of the international SCDAP Development and Training Program (SDTP)[5,6]. RELAP/SCDAPSIM uses the publicly available SCDAP/RELAP5[7,8] models developed by the US Nuclear Regulatory Commission in combination with proprietary (a) advanced programming and numerical methods, (b) user options, and (c) models developed by ISS and other SDTP members. RELAP/SCDAPSIM/MOD4.0[3], the latest in the series of SDTP-developed versions, is the first version of RELAP5 or SCDAP/RELAP5 completely rewritten to FORTRAN 90/95/2000 standards. MOD4.0 is described in a companion paper [4] and in more detail in reference [3].

As described in an earlier paper [9], the initial development and qualification of the input model for the AERE TRIGA was performed during a 3 month International Atomic Energy Agency (IAEA) internship by one of the authors (Huda). During this period, an initial set of calculations were performed with an earlier version of RELAP/SCDAPSIM/MOD3.2(am2). For this paper, additional testing and qualification of the input models and results were performed using RELAP/SCDAPSIM/MOD4.0 with the integrated RELSIM interactive simulator Graphical User Interface (GUI) [10] and uncertainty analysis package [4]. The AERE TRIGA is briefly described in Section 2. The development, qualification and application of the input model using RELAP/SCDAPSIM/MOD4.0 are presented in Sections 4 and 5.

2. Brief description of the Bangladesh AERE TRIGA

The Bangladesh TRIGA-3000, a 3MW TRIGA MARK II research reactor located near Dhaka, was commissioned in late 1986. The reactor uses a light water coolant with graphite-

reflector. It is designed for continuous operation at a steady-state power level of 3 MW (thermal). The reactor can also be operated in a pulsing mode with reactivity insertions of up to 1.4% Δk/k ($ 2.00). The reactor and experimental facilities are surrounded by a concrete shield structure. As shown in Figure 1, the reactor core and reflector assembly are located at the bottom of a 2 m diameter aluminium tank, 8.2 m deep. Approximately 6.4 m of water above the core provides vertical shielding. The TRIGA core consists of 100 fuel elements arranged in a concentric hexagonal array within the core shroud. The fuel is a solid, homogeneous mixture of Er-U-ZrH alloy.

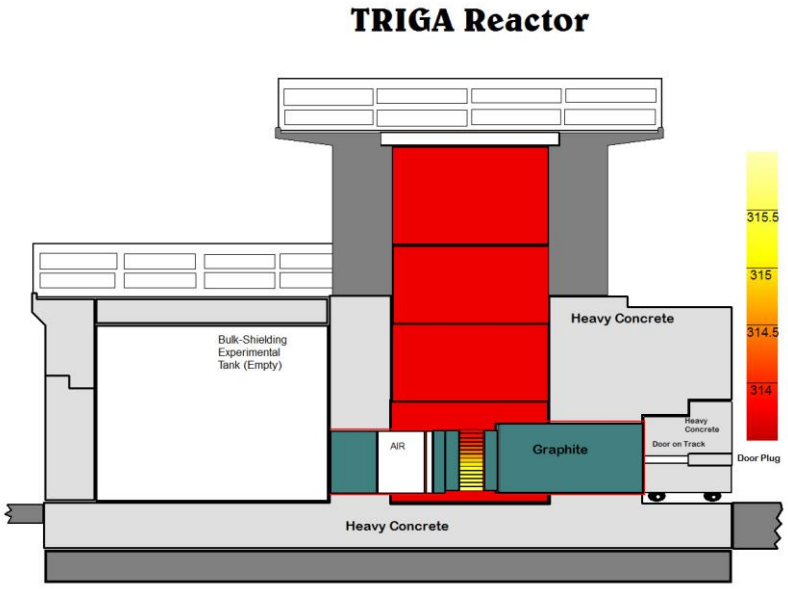

Figure 1 – TRIGA reactor tank

The reactor can be operated at power levels up to 500 kW with natural convection cooling of the core. For higher power, the forced flow mode (downward) of operation is required to transfer the reactor heat to the cooling tower. The cooling system of the TRIGA reactor is shown in Figure 2.

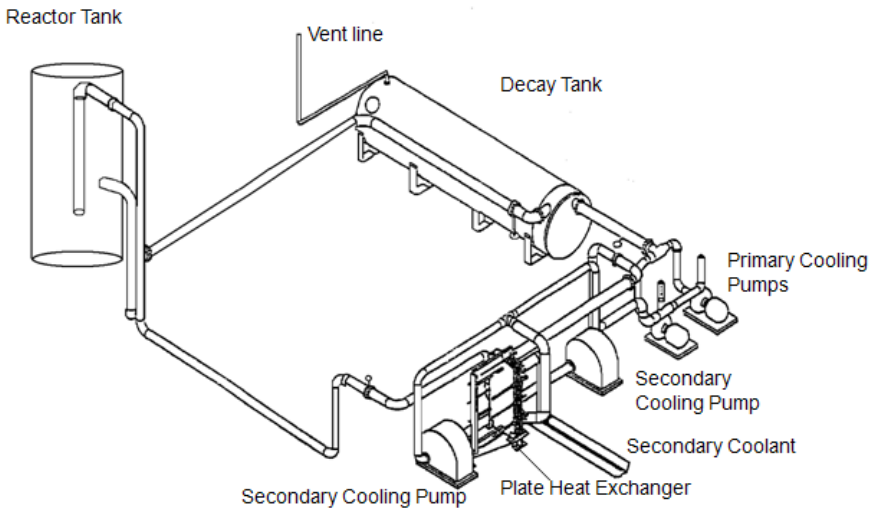

Figure 2 – TRIGA reactor cooling system

3. Development and qualification of the original RELAP/SCDAPSIM input model

As described in reference [9], the development of the preliminary input model was completed during a 3 month training fellowship supported by the IAEA. Technical support, training, and technical review of the model were performed by the ISS staff at the SDTP regional training center in Idaho. During the training period, the input model was built and tested in stages. Individual parts of the system were built and tested with simple boundary conditions. The physical arrangement was verified using the integrated 3D orthographic displays available in RELAP/SCDAPSIM. Figure 3 shows the 3D nodalization for the different components of the reactor cooling system.

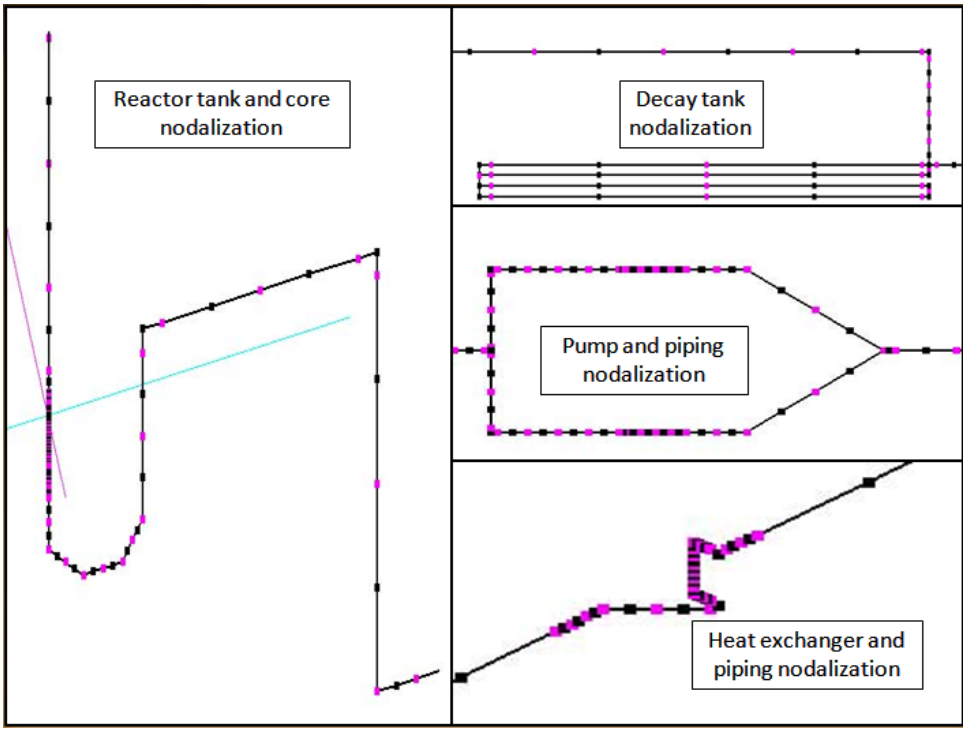

Figure 3 – TRIGA reactor cooling system components when viewed with 3D display

The 3D images for each of the four components of the cooling system shown in the figure are drawn to scale by the code using only the information included in the input model(s). The locations of each of the volumes, shown as black boxes on the figures, are drawn in reactor coordinates. The display can also be interactively rotated and scaled during the simulation to view different features of the model.

This approach was used for each of the major features of the reactor system. Then after each part of the system is tested and verified separately, the complete model was then put together as shown in figure 4. (The reactor tank and decay tanks are highlighted on the nodalization diagram and schematic.) Once the complete model was assembled, this model was then used for comparisons with plant steady state data. This comparison helped verify that the flow resistances and other model input assumptions were set properly. In addition, where available, reactor startup data or other transient data was used to verify the thermal capacitances of the system, pump coast down characteristics, and other transient characteristics of the input model. During this process the results were reviewed and any flaws in the steady state input models were corrected.

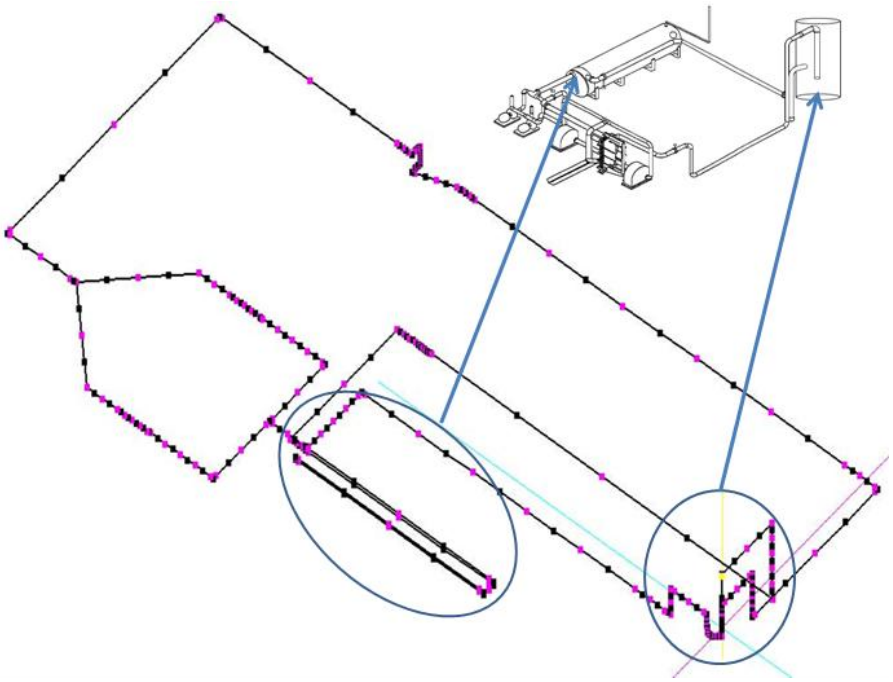

Figure 4 – Full TRIGA reactor cooling system when viewed with 3D display

4. Testing, qualification, and application of input model using MOD4.0 options

The integrated RELSIM GUI and uncertainty packages available in MOD4.0 offered unique options useful for the testing, qualification, and application of the original TRIGA input model. First, the integrated RELSIM GUI allows the user to build interactive displays that can show in detail the results of either individual components of the system or the entire system. Although the RELAP/SCDAPSIM 3D display is useful to qualify the input model and display computed results in digital form, the RELSIM GUI allows a much wider variety of displays and more complete control of the calculations. It allows the user to interactively set up accident sequences and to change the status of system components (i.e. trip a pump or open a valve). The accident progression or code calculation results can be viewed on a single or multiple monitors as shown on Figure 5. The user can then run or pause the simulation. Although the speed of the simulation will depend on the complexity of the input model and transient, typical full reactor plant models will run significantly faster than real time on current Windows PCs. (The TRIGA steady state model runs between 10-20 times faster than real time.)

The user can also build a variety of time history plot screens or data tables to display the simulation results as the simulator proceeds. The time history plots can be edited with automatically generated or user defined axes descriptions, labels, markers, legends, etc. The resulting time history plots can also be exported electronically as report ready graphs. The plot screens can be rearranged and curves and plots can be added/deleted/rearranged during the simulation.

Figures 1, 6, and 7 show three displays that were built for the TRIGA simulation. Figure 1 shows the reactor tank and core. Figure 6 shows a similar view but with some of the piping associated with the reactor tank added to the display. Figure 6 shows the inclusion of the decay tank and heat exchanger. The colors in these figures represent the fluid temperatures at different points in time during the calculations.

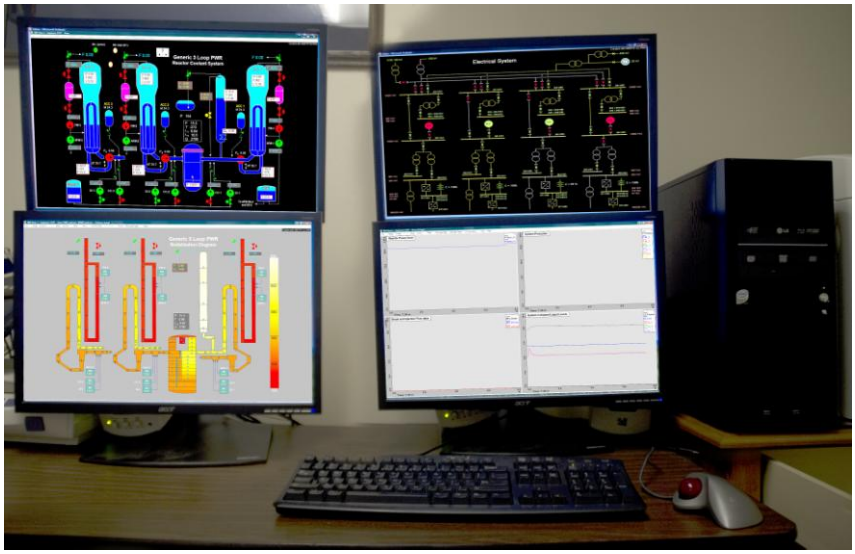

Figure 5 – Example of simulation with multiple displays on a Windows PC

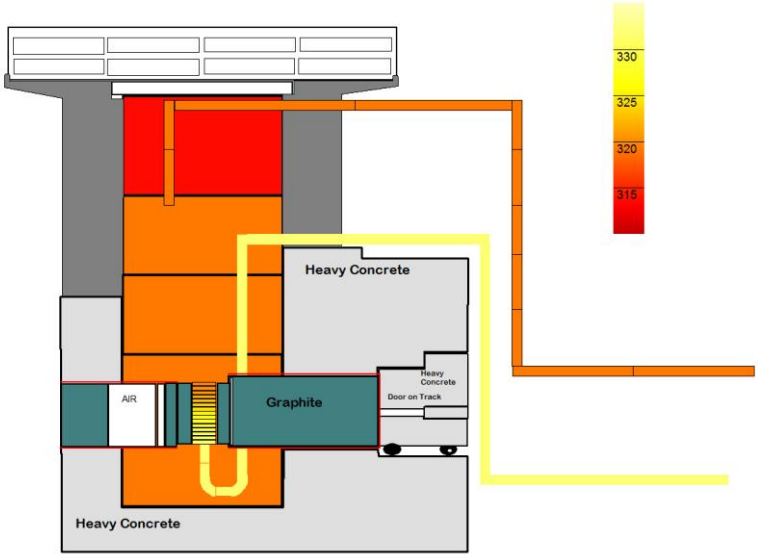

Figure 6 – RELSIM display of reactor tank, core, and associated piping fluid temperatures

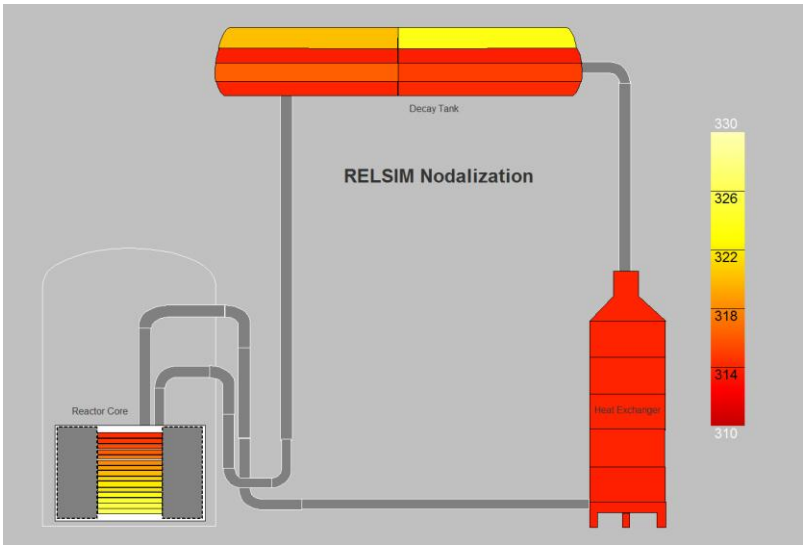

Figure 7 – RELSIM display of core, decay tank, and heat exchanger fluid temperatures

The MOD4.0 integrated uncertainty analysis package [4] can be applied to any standard RELAP5 or RELAP/SCDAPSIM input model. The user defines the code parameters that are considered to be influential in the calculations, defines their associated uncertainty distributions, and the desired output quantities with uncertainty bands. The code then uses the original input model along with the uncertainty input to generate the desired results. The uncertainty parameters that can be selected by the user can either be source code or input parameters. The source code parameters allow the user to perturb computed quantities not normally accessible through input. For example, source code parameters include:

- *Interfacial heat transfer coefficients.*
- *Heat transfer coefficients.*
- *Critical Heat Flux.*
- *Gap thermal conductivity from the gap conductance model.*
- *Viscosity.*
- *Thermal conductivity.*
- *Surface tension.*

The input parameters, as the name implies, are parameters that are defined through the input model. Examples might be boundary conditions, loss coefficients, etc. The package allows the user to easily perturb any input quantity by specifying the location in the input file (card and word number).

The user can select from a variety of PDFs and then specify the associated characteristic parameters for each parameter to be perturbed. For instance when a Normal Distribution is desired, the user must specify the mean and the standard deviation. Four types of PDFs can be selected:

- *Normal distribution.*
- *Uniform distribution.*
- *Log-normal distribution.*
- *Trapezoidal distribution.*

For the TRIGA models, it was decided to vary three source parameters to demonstrate the use of the package:

- *Liquid heat transfer coefficient $\pm$ 20%*
- *Liquid heat transfer viscosity $\pm$ 2%*
- *Liquid heat transfer thermal conductivity $\pm$ 2%*

Figure 8 shows the variation in computed steady state fluid temperatures in the core associated with variations in liquid heat transfer coefficients and fluid properties. The pink curve on the figure is the base or average fluid temperature at the bottom of the core, left axis. The green and blue curves, also left axis, represent the upper and lower bounds on the fluid temperatures at that location. As can be seen, the fluid temperatures undergo a rapid change in the first seconds as the temperatures adjust from the initial conditions, and then respond more slowly as the final steady state conditions are obtained. The variation in the liquid heat transfer coefficients and fluid properties have little impact initially but increase in influence with time. The red curve, right axis, is a plot of the difference between the upper and lower bound in fluid temperature at that location.

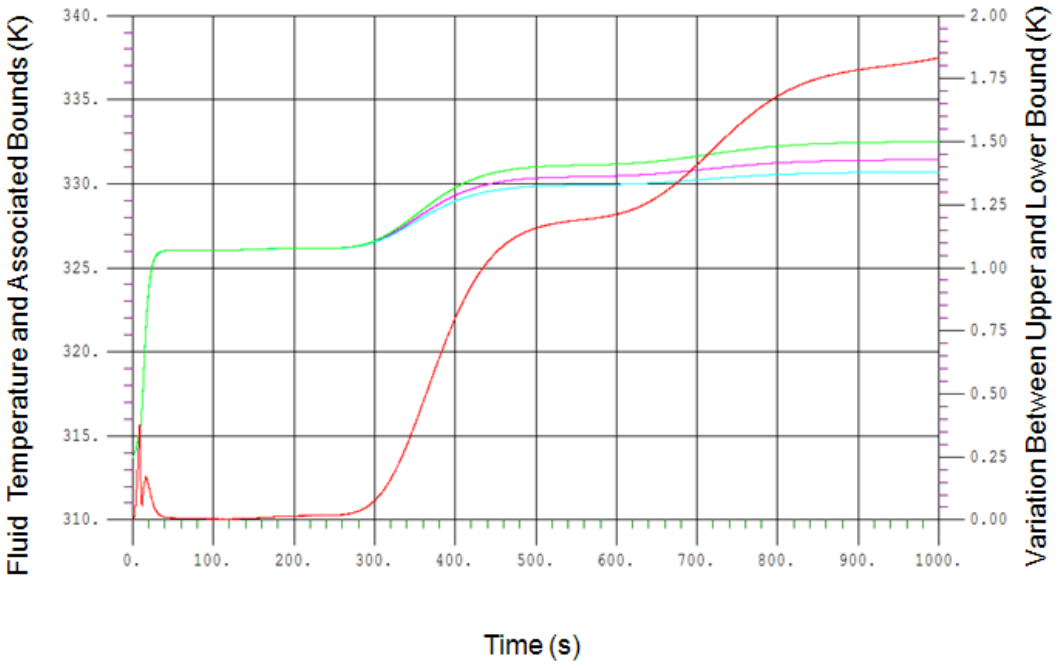

Figure 8 – Fluid temperatures at bottom of the core and associated sensitivity bounds

5. References

[1] www.relap.com.

[2] C. M Allison and J.K Hohorst, "Role of RELAP/SCDAPSIM in Nuclear Safety", International Topical Meeting on Safety of Nuclear Installations, Dubrovnik, Croatia, September 2008.

[3] C. M. Allison, R. J. Wagner, L.J.Siefken, J.K. Hohorst, "The Development of RELAP5/SCDAPSIM/MOD4.0 for Reactor System Analysis and Simulation", Proceedings of the 7th International Conference on Nuclear Option in Countries with Small and Medium Electricity Grids, Dubrovnik, Croatia, (May 2008).

[4] C. M. Allison, J. K. Hohorst, M. Perez, and F. Reventos, "Application of RELAP/SCDAPSIM with Integrated Uncertainty Options to Research Reactor Systems Thermal Hydraulic Analysis", RRFM 2010, Marrakech, Morocco, March 21-25, 2010.

[5] www.sdtp.org.

[6] C. M Allison and J.K Hohorst, "SDTP—Developing Technology for the Nuclear Industry", 13th International Conference on Nuclear Engineering, ICONE13-50979, Beijing, China, May 16–20, 2005.

[7] RELAP5 Code Development Team, "RELAP5/MOD 3.3 Code Manual, Vol. 1-8", NUREG/CR-5535/Rev1 (December, 2001).

[8] SCDAP/RELAP5 Development Team, "SCDAP/RELAP5/MOD3.2 Code Manual, Vol. 1-5", NUREG/CR-6150, INEL-96/0422, (July, 1998).

[9] A. R. Antariksawan, M. Q. Huda, Tiancai Liu, J. Zmitkova, C. M. Allison and J. K. Hohorst, "Validation of RELAP/SCDAPSIM/MOD3.4 for Research Reactor Applications", *Proc. Intl. Conf. on Nucl. Eng.,* ICONE13-50124, Beijing, China, May 16-20, 2005.

[10] C. M. Allison, B. S. Allison, U. Luettringhaus, J. K. Hohorst, "Application of RELSIM-RELAP/SCDAPSIM for University Training and Simulator Development", Proceedings of the 18th International Conference on Nuclear Engineering, ICONE18, Xi'an China, May 17-21, 2010.

NEUTRONICS MODELING OF TRIGA REACTOR AT THE UNIVERSITY OF UTAH USING AGENT, KENO6 AND MCNP5 CODES

XUE YANG[1], SHANJIE XIAO[2], DONGOK CHOE[2], TATJANA JEVREMOVIC[2]
[1]School of Nuclear Engineering, Purdue University
400 Central Dr, West Lafayette, IN, 47907 – USA
[2]Utah Nuclear Engineering Program, The University of Utah
50 S. Central Campus Dr, Salt Lake City, UT, 84112 – USA

ABSTRACT

The TRIGA reactor at the University of Utah is modelled in 2D using the AGENT state-of-the-art methodology based on the Method of Characteristics (MOC) and R-function theory supporting detailed reactor analysis of reactor geometries of any type. The TRIGA reactor is also modelled using KENO6 and MCNP5 for comparison. The spatial flux and reaction rates distribution are visualized by AGENT graphics support. All methodologies are in use in to study the effect of different fuel configurations in developing practical educational exercises for students studying reactor physics. At the University of Utah we train graduate and undergraduate students in obtaining the Nuclear Regulatory Commission license in operating the TRIGA reactor. The computational models as developed are in support of these extensive training classes and in helping students visualize the reactor core characteristics in regard to neutron transport under various operational conditions. Additionally, the TRIGA reactor is under the consideration for power uprate; this fleet of computational tools once benchmarked against real measurements will provide us with validated 3D simulation models for simulating operating conditions of TRIGA.

1. Introduction

1.1 TRIGA reactor at the University of Utah

The University of Utah has a 100 kW pool type TRIGA reactor. Seven rings of fuel elements form the core in a triangular-pitched array. The current core configuration is depicted in Fig 1. Three types of fuel with different burn-up along with graphite, water, heavy water and control rod cells are placed in an unsymmetrical configuration to efficiently utilize the fast and thermal neutron yield. For simplicity, the irradiation facilities surrounding the core are not modelled and the cylinder tank filled with water is approximated by a hexagonal prism[1].

1.2 Computational Tools

The TRIGA reactor was modelled using the following four transport codes: DRAGON [1], AGENT [2], KENO6 [3] and MCNP5 [5]. DRAGON is developed by Polytechnique Montréal and contains a various methods to simulate a fuel assembly. The primary methodology of DRAGON is a collision probability method. In this paper, DRAGON is used to read microscopic cross section library and perform self-shielding calculation to produce broad group cross sections for AGENT. AGENT (Arbitrary GEometry Neutron Transport) is the state-of-the-art code currently maintained by Advanced Radiation Simulation Laboratory (ARSiL) at The University of Utah. AGENT methodology is based on the Method of Characteristics (MOC) and R-function theory supporting detailed reactor analysis of reactor geometries of any type. Oak Ridge National Laboratory (ORNL) and Los Alamos National Laboratory (LANL) developed the KENO6 and MCNP5 code, respectively; KENO is the primary criticality analysis module in SCALE5.1 code system [5]. Because of the triangular-pitched array of TRIGA reactor, KENO6

[1]Our next simulation model will include full 3D real geometry model of the TRIGA core and the cylinder tank.

is selected instead of KENO5 to be able to model more complex geometry. Both KENO6 and MCNP5 are 3D Monte Carlo codes, but KENO, specifically designed for reactor modelling, relies on other SCALE modules, such as BONAMI/CENTRUM/PMC, to produce resonance corrected cross section prior to KENO calculation, while MCNP5 could account for the real physics processes and could be used for general purposes. The AGENT code can be used to model 2D or 3D cores based on the MOC.

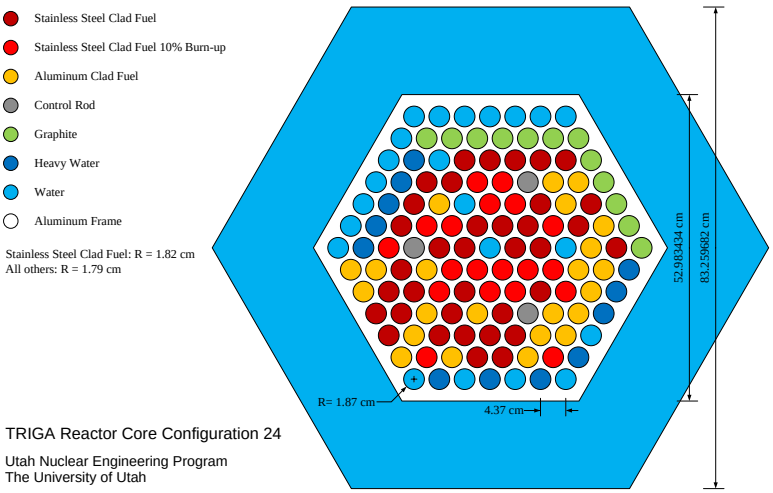

Figure 1. TRIGA core configuration

2. Processing the Cross Sections Using DRAGON

The standard microscopic cross section library of DRAGON consists of 69 groups or 172 groups WLUP library [6] and most of the common nuclide data are based on the ENDF/B-VI.8. Because the Zr-ZrH_2 data is not available in WLUP library and due to an uncertainty of the H-ZrH_2 data (We performed a TRIGA unit cell calculations, using H-ZrH_2 and that resulted in up to 2.4% k-inf overestimation by DRAGON compared to KENO6), the H1 and Zr-natural are selected in all of the presented calculations for fair inter-comparison.

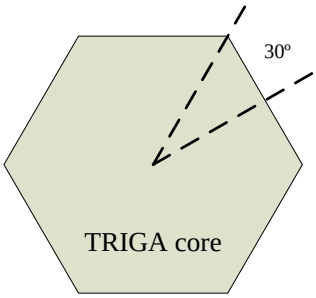

Figure 2. 1/12 TRIGA core modelled in DRAGON

Because of the large number of zones and unsymmetrical configuration of the TRIGA core, DRAGON could not explicitly perform full core calculation. A 1/12 cut of the core (Fig 2) with minor modification to include all cell types is used in DRAGON calculation. Seven groups flux weighted isotropic cross sections are collapsed from 172 groups WLUP library by DRAGON. The energy group structure is identical to C5G7 benchmark [7], but the energy group limit is changed to the nearest energy group limit found in 172 groups WLUP library. Table 1 lists the group structure used in DRAGON to collapse the cross sections for AGENT. The first two groups are fast groups, and the next two groups fall into the resonance region. The last three groups are thermal energy groups.

Table 1. Energy range of seven group cross section

Group index	Energy range (eV)
1	$1.35335\times10^{6} \rightarrow 1.96403\times10^{7}$
2	$9118.82 \rightarrow 1.35335\times10^{6}$
3	$55.5951 \rightarrow 9118.82$
4	$4.0 \rightarrow 55.5951$
5	$0.625 \rightarrow 4.0$
6	$0.134 \rightarrow 0.625$
7	$10^{-5} \rightarrow 0.134$

In the DRAGON model, it is important to define multiple mixture indices for the same material that appears in different fuel cells. For example, aluminium serves as moderator surrounding all three types of fuel, and three mixtures with identical composition should be defined and treated as different mixtures after the self-shielding calculation and the collapse of cross sections. The cross section pre-processors of SCALE5.1 use similar idea to produce the corrected cross sections.

3. 2D TRIGA core modelling using AGENT, KENO6 and MCNP5

To coordinate with WLUP library, KENO6 simulation uses 238 groups ENDF/B-VI library and MCNP5 uses continuous energy ENDF/B-VI library. The calculation parameters are summarized in Table 2. Figure 3 illustrates the sub mesh pattern used in AGENT for a typical hexagonal unit cell. The dash lines and the material interface define the subdivisions, whichmaximum area in the core region is $0.96cm^2$. The AGENT parameters are selected such to provide a good resolution yielding accurate estimate of the multiplication factor and reaction rates. 100 millions neutrons are simulated by both Monte Carlo codes to lower the standard deviation to below 10^{-4}. All sides of the core are set to free boundary conditions, and the top and bottom boundary conditions are set to reflective in all three models. Additionally, all three B_4C control rods are withdrawn, and the control rod spaces are filled with the water.

Table 2. Calculation parameters of AGENT, KENO6 and MCNP5

	AGENT	KENO6	MCNP5
Library	7g collapsed from 172g WLUP	238g ENDF/B-VI	ENDF/B-VI
Neutrons	NA	100 millions	100 millions
k-eff and flux criteria	10^{-5} and 10^{-4}	NA	NA
Azimuthal angles	36	NA	NA
Ray separation	0.02cm	NA	NA
Edges	4 per segment / 264 in total	NA	NA
Sub mesh	6 triangles per hexagon lattice. Fuel pin is divided into 3 rings Total zones: 9414	Total zones: 349	Total zones: 184

The effective multiplication factor and runtime are summarized in Table 3. AGENT and KENO6 multiplication factors are very close, indicating that codes using resonance corrected cross sections based on multi-group cross section library are consistent with each other. Compared to MCNP5, both AGENT and KENO6 slightly underestimate the k-eff for about 0.4%. The reason for this difference lies in the ways cross sections are corrected and because the libraries are different; the continuous energy MCNP5 avoids many of the assumptions inherent in a multi-group treatment [8]. Since the available KENO6 and MCNP5 codes are serial, AGENT calculation does not exploit high efficiency with parallel computing on multiprocessor server. For this complex geometry, AGENT spent half an hour to analyze the geometry and another two hours to complete the MOC iteration, while the Monte Carlo codes require 20

hours for 100 million particle simulations. Therefore, deterministic methodology still plays an important role in the field of reactor analysis for the short computation time with good accuracy.

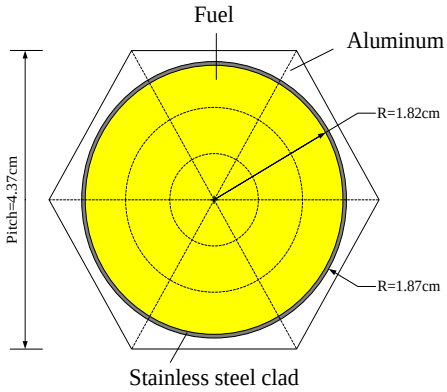

Figure 3. AGENT sub mesh pattern for a typical hexagonal fuel cell

Table 3. k-eff and calculation time

	AGENT	**KENO6**	**MCNP5**
k-eff	1.02188	1.02182±0.00008	1.02576±0.00007
k-eff relative DIFF	-0.38%	-0.38%	----
Runtime (hours)	Total: 2.5 / MOC: 2.0	20.6	18.3
CPU models	INTEL XEON 5520	INTEL Q6600	INTEL Q6600
Machine	LINUX	WinXP SP3	WinXP SP3

As shown in Fig 4, the seven group scalar flux, fission rate and absorption rate distributions are created from the AGENT simulation. The flux has more of an elliptical shape, because the lower right corner and upper left corner of the core are filled with water and heavy water region. The highest thermal flux is obtained in the centre irradiation chamber that is filled with water, while the highest fast flux appears in the second ring surrounding the centre irradiation chamber.

4. Conclusion and future work

The TRIGA reactor at the University of Utah is modelled using AGENT, KENO6 and MCNP5 codes in 2D. The acquired AGENT multiplication factor is very close to KENO6 and acceptably compares to MCNP5. Good AGENT computational efficiency and high quality visualization can show details of TRIGA flux and reaction rates distribution. This calculation is used in our research but also in education as a part of some of our ongoing courses. The next step is to use AGENT to examine the anisotropic effect and model our TRIGA core in 3D.

5. References

[1] G. Marleau, A. Hébert and R. Roy, *A User Guide for DRAGON 3.06, Report IGE-174 Rev. 7*, Institut de génie nucléaire, École Polytechnique de Montréal, Montréal, Québec (2000).

[2] T. Jevremovic, M. Hursin and S. Xiao, Synergism of The Method of Characteristic, R-Functions and Diffusion Solution for Accurate Representation of 3D Neutron Interactions in Research Reactors Using the AGENT Code System, *Annals of Nuclear Energy*, **33**(13), 1116-1133 (2006).

[3] D. F. Hollenbach, L. M. Petrie and N. F. Landers, *KENO-VI: A General Quadratic Version of the KENO Program, ORNL/TM-2005/39, Version 5.1, Vol. II, Book 3, Sect. F17*, Oak Ridge National Laboratory, Oak Ridge, Tennessee (2006).

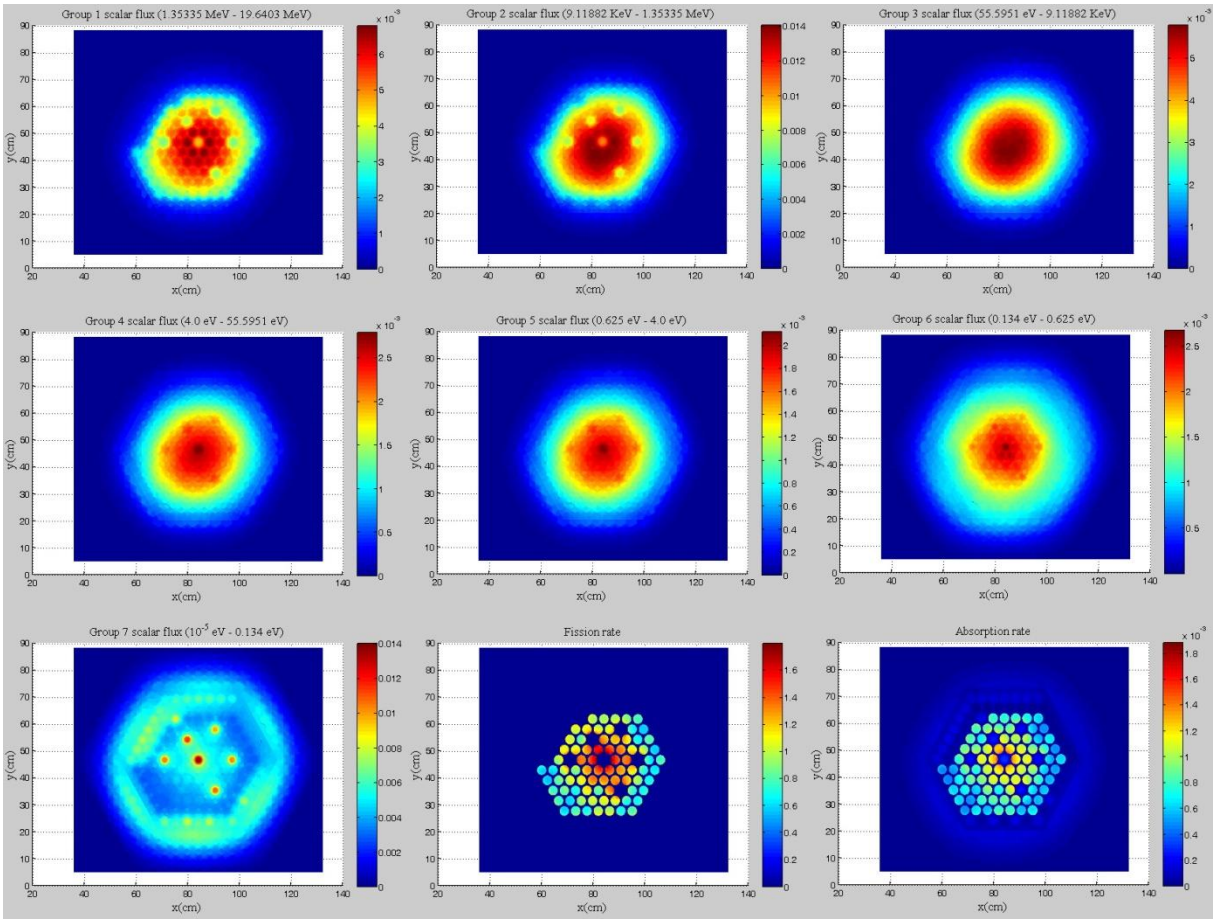

Figure 4. AGENT simulated TRIGA scalar flux, fission rate and absorption rate profiles

[4] X-5 Monte Carlo Team, *MCNP — A General Monte Carlo N-Particle Transport Code, Version 5, LA-UR-03-1987*, Los Alamos National Laboratory, Los Alamos, New Mexico (2005).

[5] *SCALE: A Modular Code System for Performing Standardized Computer Analyses for Licensing Evaluation*, *ORNL/TM-2005/39, Version 5.1*, Vols. I-III, Oak Ridge National Laboratory, Oak Ridge, Tennessee (2006).

[6] *WIMS-D Library Update*, International Atomic Energy Agency, Vienna (2007).

[7] Organization for Economic Co-operation and Development (OECD), *Benchmark on Deterministic Transport Calculations without Spatial Homogenisation: MOX Fuel Assembly 3-D Extension Case*, Nuclear Energy Agency (2005).

[8] Mark D. DeHart and Sedat Goluoglu, Keno Continuous Energy Calculations for A Suite of Computational Benchmarks for the Doppler Reactivity Defect, *Joint International Topical Meeting on Mathematics & Computation and Supercomputing in Nuclear Applications (M&C + SNA 2007)*, Monterey, California, April 15-19, 2007, on CD-ROM, American Nuclear Society, LaGrange Park, IL (2007)

ACCIDENT SCENARIOS OF THE TRIGA MARK II REACTOR IN VIENNA

M. VILLA, H. BÖCK, M. HAYDN
Vienna University of Technology, Atomic Institute
Stadionallee 2, 1020 Wien, Austria

ABSTRACT

The safety report of the TRIGA Mark II reactor in Vienna includes three accident scenarios and their deterministic dose consequence to the environment. The destruction of the most activated fuel element, the destruction of all fuel elements and a plane crash were treated scenarios in that report. The calculations were made in 1978 with the computer program STRISK. In this work, the program package PC COSYMA was applied on the TRIGA Mark II reactor in Vienna and the deterministic consequences of the scenarios to the environment were updated. The fission product inventories of all fuel elements were taken from a calculation with ORIGEN2. To get meteorological data of the atmospheric condition around the release area, a weather station was installed. The release parameters were taken from the safety report or were replaced by worst case parameters. Further on, a fourth scenario for the case of a small plane crash was added. For the sake of completeness all scenarios were calculated with different atmospheric conditions. In this paper only two accident scenarios are presented, the destruction of the fuel element with the highest activity content and the case of a large plane crash, which means a totally destruction of the reactor hall.

1. Introduction

The program system PC-Cosyma Version 2.01 was used to assess the off-site consequences of an accidental release of radioactive material into the atmosphere. In this paper the effective dose (ICRP-60) after one day and after 50 years of two scenarios are treated. These scenarios are the destruction of the fuel element with the highest activity and the case of a big plane crash with totally destruction of the reactor hall. The evaluations were made deterministic, which means the atmosphere was temporal stable. The atmospheric condition E was used, which means a stable atmosphere. Standard values for mixing layer height (320 m), wind profile exponent (p = 0,44) and sigma coefficients were used for calculation. A list of used deposition parameters (standard values of PC-Cosyma) see table 1.

Only noble gases and halogens are volatile enough to release into the atmosphere and only nuclides with a half live higher than 14.1 minutes were treated. In this work only one release phase is used with a release duration of one hour and no thermal energy was assumed (0 MW). The fission product inventories of all fuel elements were taken from a calculation with ORIGEN2 whereas the inventory of each fuel element was evaluated for a reactor operation from March 9, 1962, to June 30, 2009. After destruction of an fuel element, only a fraction of the whole inventory is released. To define the fraction of the released noble gases and halogens, the formula $w_i = e_i \cdot f_i \cdot g_i$ was used, whereas e_i defines the fraction of fission products, which migrate into the gap between fuel and fuel element cladding and was empirically found by general atomics with a value of 1.5×10^{-3} percent. f_i defines the fraction of the fission products, which migrate from the gap between fuel and fuel element cladding into the water tank. g_i defines the fraction of fission products, which are released from the water tank to the ventilation system or into the atmosphere. In the further paper index *N* is used for noble gases and the index *H* is used for halogens.

The received dose outdoors is higher than the received dose in a protected location, because shielding effects occur. A list of used shielding effects see table 2. All scenarios were calculated within 5 km from the release point. The lattice is partitioned into 64 sectors and 25 circles.

aerosols	dry deposition velocity [m/s]	0.001
	dry deposition correction factor	1
	wet deposition coefficient a	8.0E-05
	wet deposition coefficient b	0.8
elementary bound iodine	dry deposition velocity [m/s]	0.01
	dry deposition correction factor	1
	wet deposition coefficient a	8.0E-05
	wet deposition coefficient b	0.6
organically bound iodine	dry deposition velocity [m/s]	5.0E-004
	dry deposition correction factor	1
	wet deposition coefficient a	8.0E-07
	wet deposition coefficient b	0.6

Tab 1: Used deposition parameters

cloud radiation	1
ground radiation	1
inhalation	1
re suspension	1
deposition on skin and clothes	1

Tab 2: Used shielding parameters

2. Worst case scenario 1 - Destruction of the fuel element with highest activity content

In scenario 1 it was assumed, that the building is alright. The dimensions of the building were assumed as follows: height 20 m, width 20m and the release height was also assumed with 20 m. The fission product inventory of the fuel element with the highest activity content was evaluated with ORIGEN [7] and is tabulated in table 3 (only nuclides, which were considered in PC COSYMA).
For e_N, f_N and g_N the same assumptions were used as in the safety report [8]. e_N is the empirically found parameter from General Atomic and describes the amount of noble gases, which reach the gap between fuel and fuel element cladding. It was assumed, that 100% of all noble gases were released from the gap between fuel and fuel element cladding into the water tank. Further was assumed that all noble gases from the water tank were released to the ventilation system.
For e_H, f_H and g_H the same assumptions were used as in the safety report [8]. e_H is the empirically found parameter from General Atomic and describes the amount of halogens, which reach the gap between fuel and fuel element cladding. It was assumed that 50% of all halogens were released from the gap between fuel and fuel element cladding into the water tank. It was assumed that 10% of all halogens in the water tank were in organic form and were released to the ventilation system. Further was assumed that 1% of the leftover halogens in the water tank (which had another chemical form) were released to the ventilation system. In table 4 a list of the release fractions for noble gases, organically bound halogens, halogens in other chemical form and the total release fractions are presented.

	Activity [Bq]		Activity [Bq]
Kr-83m	$5.91 \cdot 10^{10}$	I-133	$7.44 \cdot 10^{11}$
Kr-85m	$1.39 \cdot 10^{11}$	I-134	$8.40 \cdot 10^{11}$
Kr-85	$2.22 \cdot 10^{10}$	I-135	$6.93 \cdot 10^{11}$
Kr-87	$2.81 \cdot 10^{11}$	Xe-131m	$3.56 \cdot 10^{9}$
Kr-88	$3.97 \cdot 10^{11}$	Xe-133m	$2.18 \cdot 10^{10}$
I-129	$7.47 \cdot 10^{4}$	Xe-133	$7.45 \cdot 10^{11}$
I-130	$7.16 \cdot 10^{8}$	Xe-135m	$1.26 \cdot 10^{11}$
I-131	$3.21 \cdot 10^{11}$	Xe135	$7.03 \cdot 10^{11}$
I-132	$4.77 \cdot 10^{11}$	Xe-138	$6.87 \cdot 10^{11}$

Tab 3: Volatile fission product inventory of fuel element 10075

	Noble gases	Organically halogens	Other halogens
e	$1.5 \cdot 10^{-5}$	$1.5 \cdot 10^{-5}$	$1.5 \cdot 10^{-5}$
f	1	0.5	0.5
g	1	0.1	0.009
w	$1.5 \cdot 10^{-5}$	$7.5 \cdot 10^{-7}$	$6.75 \cdot 10^{-8}$

Tab 4: Release fractions of scenario 1

The only halogen, which was used in the calculation was iodine. In PC COSYMA, isotopes of iodine are partitioned into three chemical forms. These are organically bound iodine, elementary bound iodine and aerosol iodine. It was assumed that 92% of the released iodine was organically bound and 8% was in other chemical form. Further was assumed, that the other iodine was partitioned into 50% of elementary bound iodine and 50% of iodine in aerosol form.
For this calculations, a Pasquill stability class E and a wind speed of 1 m/s was used as worst case atmospheric condition. Because of measurements with the weather station a wind direction from WNW and no rain were used. The dose is evaluated in an area within 5 km distance from the release point (Atomic Institute).
The maximum effective dose (ICRP-60) in Sv after one day has a value of $2.51 \cdot 10^{-10}$ Sv and lies in wind direction close to the releasepoint. Exterior a radius of 0.31 km the dose is less than $1 \cdot 10^{-10}$ Sv and exterior a radius of 1.98 km the dose is less than $1 \cdot 10^{-11}$ Sv.
The maximum effective dose (ICRP-60) in Sv after 50 years has a value of max. $7.73 \cdot 10^{-10}$ Sv and lies in wind direction close to the releasepoint. Exterior a radius of 0.60 km the dose is less than $1 \cdot 10^{-10}$ Sv and exterior a radius of 3.36 km the dose is less than $1 \cdot 10^{-11}$ Sv.

3. Worst case scenario 2 - Case of a large plane crash

In this scenario the case of a large plane crash was regarded. It was assumed, that the building was fully damaged. The height of the building was assumed with 1 m, the width with 20 m and the release height was assumed with 1 m. The fission product inventory of the whole reactor core (summed over all fuel elements) is presented in table 5 (only nuclides which were considered in the calculation).
For e_N, f_N and g_N the same assumptions were used as in the safety report [8]. e_N describes the amount of noble gases, which reach the gap between fuel and fuel element cladding and has the value 1. This means, it was assumed that all noble gases reach the gap between fuel and fuel element cladding. Further was assumed that 100% of all noble gases were released from the gap between fuel and fuel element cladding into the water tank and all noble gases from the water tank were released into the atmosphere.

	Activity [Bq]		Activity [Bq]

Kr-83m	$3.82 \cdot 10^{12}$	I-133	$4.83 \cdot 10^{13}$
Kr-85m	$9.00 \cdot 10^{12}$	I-134	$5.45 \cdot 10^{13}$
Kr-85	$1.67 \cdot 10^{12}$	I-135	$4.49 \cdot 10^{13}$
Kr-87	$1.82 \cdot 10^{13}$	Xe-131m	$2.30 \cdot 10^{11}$
Kr-88	$2.57 \cdot 10^{13}$	Xe-133m	$1.41 \cdot 10^{12}$
I-129	$8.78 \cdot 10^{6}$	Xe-133	$4.83 \cdot 10^{13}$
I-130	$6.57 \cdot 10^{10}$	Xe-135m	$8.19 \cdot 10^{12}$
I-131	$2.08 \cdot 10^{13}$	Xe135	$4.59 \cdot 10^{13}$
I-132	$3.10 \cdot 10^{13}$	Xe-138	$4.45 \cdot 10^{13}$

Tab 5: Whole reactor inventory of volatile fission products

For e_H, f_H and g_H the same assumptions were used as in the safety report [8]. e_H is the empirically found parameter from General Atomic and describes the amount of halogens, which reach the gap between fuel and fuel element cladding. The safety report [8] partitioned halogens into two classes, organic halogens and other halogens. In this report it was assumed that 100% of all halogens were released from the gap between fuel and fuel element cladding into the water tank. It was assumed that 100% of all halogens in the water tank were released into the atmosphere. Further was assumed, that 10% of all halogens were in organic form and the rest was in other form. In table 4 a list of release fractions for organically bound halogens, halogens in other chemical form and noble gases is presented.

	Noble gases	Organically halogens	Other halogens
e	1	$1.5 \cdot 10^{-5}$	$1.5 \cdot 10^{-5}$
f	1	1	1
g	1	0.1	0.9
w	1	$1.5 \cdot 10^{-6}$	$1.35 \cdot 10^{-5}$

Tab 6: Release fractions of scenario 4

In the safety report [8] it was assumed that 10% of the released iodine was organically bound and 90% was in other form. Further was assumed that 50% of the other iodine was elementary bound iodine and 50% was in aerosol form.
For these calculations, Pasquill stability class E and a wind speed of 1 m/s were used as worst case atmospheric conditions. Because of measurements with the weather station a wind direction from WNW and no rain were used. The dose is evaluated in an area within 5 km distance from the release point (Atomic Institute).
The maximum effective dose (ICRP-60) in Sv after one day has a value of max. $3.72 \cdot 10^{-4}$ Sv and lies in wind direction close to the release point. Exterior a radius of 0.60 km the dose is less than $1 \cdot 10^{-4}$ Sv and exterior a radius of 4.38 km the dose is less than $1 \cdot 10^{-5}$ Sv.
The maximum effective dose (ICRP-60) in Sv after 50 years has a value of max. $3{,}74 \cdot 10^{-4}$ Sv and lies in wind direction close to the release point. Exterior a radius of 0.60 km the dose is less than $1 \cdot 10^{-4}$ Sv and exterior a radius of 4.38 km the dose is less than $1 \cdot 10^{-5}$ Sv.

4. References

[1] National Radiological Protection Board, Forschungszentrum Karlsruhe GmbH; EUR 16240 - PC Cosyma (Version 2.0) User Guide; Luxembourg 1995

[2] J.A. Jones, P.A. Mansfield, S.M. Haywood, I. Hasemann, C. Steinhauer, J. Erhardt, D. Faude; EUR 16329 - PC Cosyma (Version 2): An accident consequence assessment package for use on a PC; Office for Official Publications of the European Communities; Luxembourg 1996

[3] M. Strubegger; STRISK. Ein Programm zur Berechnung der radiologischen Konsequenzen nach kurzfristigen Emissionen radioaktiver Stoffe aus kerntechnischen Anlagen; Diplomarbeit am Atominstitut der Österreichischen Universitäten; Wien 1978
[4] W. Kirsch; Vorbereitungspraktikum über Kernspaltung; Die Anwendung des Programmpakets COSYMA auf den Forschungsreaktor TRIGA MARK II; Wien 1998
[5] K. H. Lieser; Nuclear and Radiochemistry - Fundamentals and Applications; Second, Revised Edition; WILEY-VCH 2001
[6] S. Ludwig; Revision to ORIGEN2 - Version 2.2; Oak Ridge National Laboratory, 2002
[7] R. Khan; MCNP core calculation of the TRIGA Mark II reactor at the Atomic Institute Vienna; PhD at Vienna University of Technology; in progress
[8] Sicherheitsbericht des Atominstituts, AIAU 26314; Dez. 2006
[9] H. Böck, M. Haydn; Accident scenarios with environmental impact of the TRIGA Mark II reactor in Vienna; Diploma Theses; Vienna University of Technology, Atomic Institute; September 2009
[10] H. Böck, M. Villa; The TRIGA Mark-II Reactor; Vienna University of Technology, Vienna, Austria (private communication)

FEASIBILITY STUDY OF THE UNDERWATER NEUTRON RADIOGRAPHY FACILITY USING THE UNIVERSITY OF UTAH 100 KW TRIGA (UUTR) REACTOR

DONGOK CHOE[1], XUE YANG[2], SHANJIE XIAO[1], TATJANA JEVREMOVIC[1]
[1]*Utah Nuclear Engineering Program, The University of Utah*
50 S. Central Campus Dr, Salt Lake City, UT, 84112 – USA
[2]*School of Nuclear Engineering, Purdue University*
400 Central Dr, West Lafayette, IN, 47907 – USA

ABSTRACT

The University of Utah 100 kW TRIGA (UUTR) reactor provides usable neutron yields for neutron radiography. Currently, UUTR reactor has three irradiators (Central, Pneumatic, and Thermal irradiators) and one Fast neutron Irradiation Facility (FNIF). These irradiators are very small so they are not suitable for neutron radiography. UUTR has three beam ports but they are not available due to the structure of the core. All sides of the core are occupied by FNIF, Thermal Irradiator, and three ion chambers. The only available position for underwater vertical beam port is on the top of the FNIF. There are two factors necessary to fulfill to be able to realize vertical underwater beam port: noninterruption to other facilities and radiation shielding. Designing the vertical beam port as movable ensures good access to the core and pool, while still providing a good neutron radiography environment. Keeping the top of the beam port below the surface of the pool the water represents biological shield. Neutron radiographs, with a simple setup of efficient neutron converters and digital camera systems, can produce acceptable resolution with an exposure time as short as a few minutes. It is important to validate the design with calculations before constructing the beam port. The design of the beam port is modeled using the MCNP5 transport code. A minimum of 10^5 neutrons/cm^2-sec thermal neutron flux is required for high resolution neutron radiography. Currently, the UUTRIGA is in the process of upgrading its power from 100 kW to 250 kW. Upon the completion of the upgrading, the maximum neutron flux in the core will be ~$7x10^{12}$ neutrons/cm^2-sec. This paper discusses a modeling and evaluation of reactor's capability for a neutron radiography facility.

Key words: Neutron radiography, research reactor, MCNP5, beam port

1. Introduction

X-ray radiography has a long history of applications in medicine as well as in the field of nondestructive testing. However, X-ray radiography images are created with a markedly different image that can be detected through neutron radiography. Neutron radiography is a nondestructive testing technique as well, but allows imaging of otherwise undetectable inside-defects in a variety of materials such as turbine blades, crank axis, and automobile batteries. Neutron radiography can detect any hints of corrosion or cracks inside of metallic structures [1]. The University of Utah has a 100 kW TRIGA reactor (UUTR). The UUTR core is based on a hexagonal prism lattice with a spacing of 1.72 inches (4.37cm) center to center. The core has seven rings of fuel elements marked as A-ring, B-ring, up to G-ring. The A-ring is actually not a ring since it has only one space position and is located at the center of the core; it does not contain any fuel. This is the location of the highest flux in the core and this space is available for

irradiating the samples. The B-ring (outside of the A-ring) consists of six fuel element locations; each ring outside of the previous has an increased number of assembly and fuel element locations by six. The core is not loaded in a uniform manner due to the types of irradiation facilities present. The Thermal Irradiator (TI) has graphite reflector elements located in G2 through G7. The TI tank is filled with D_2O and has a sample insertion tube extending from the center of the TI to the top of the reactor pool. The Fast Neutron Irradiation Facility (FNIF) is intended to provide a neutron spectrum approximating a fission spectrum. It is placed as close as possible to the outer ring of fuel with as little moderation as possible. The FNIF has an insertion location, which is surrounded by two inches of solid lead to decrease the gamma irradiation while not moderating the neutrons significantly. The UUTR tank was designed with the ability to add beam ports at three different locations around the core [5]. The design incorporated outer beam port tubes extending down through the floor, through the outer steel tank, and abutted against the inner aluminum tank. The angle is such that a beam port insert could be lowered into the pool and placed against the core on one end and against the inner aluminum tank on the other end lined up with the outer beam port tube. The design of the insert would need to be such that it has slight negative buoyancy. The advantage of the beam port is that the beam port insert could be moved or removed when it is not in use, providing a better access to the core, and more flexibility for users of the facilities. Issues with the design required to be resolved include the biological shield needed at the outer end of the beam port, the location of various equipment around the outside of the pool and core, and the right angle of the beam. Because of the location of the ports around the outside of the pool, the space available for experiments and the biological shield are extremely limited. The three outer ports are located on 120° intervals around the outside of the pool with the ports pointing directly north, southwest, and southeast. The smallest available space around the reactor pool is directly north while the largest space is southwest. This space issue renders the north port completely unusable while the southwest and southeast ports have limited space due to the east and west walls of the reactor room. The core would also need to be changed to move instrumentation or existing experimental facilities out of the way of the beam port insert. The angled beam port would create difficulties in performing certain experiments such as neutron radiography. The difficulties could likely be overcome, but may require extravagant engineering solutions. These challenges pointed out in examining the vertical beam port to alleviate some of the issues as discussed. If the vertical beam port is designed as moveable, it can provide good access to the core and pool while providing a good neutron radiography environment. If the top of the beam port is kept below the surface of the pool, the water above the port will act as a good biological shield.

2. Efficient UUTR Beam Port Design

Placement of the vertical beam port can have a drastic effect on the beam port flux, reactor operation, and the usability of facilities. A beam port placed directly over the center of the core would maximize the neutron flux in the beam port. However, this configuration would interfere with control rod drive mechanism and visual inspections of the core. It would also hamper access to some of the other experimental facilities decreasing or eliminating the opportunities for piggybacking experiments thus increasing the operating costs of the reactor. Placement of the vertical beam port to the side of the core will lower the beam flux but it does not require changes to the control rod drive mechanism and provides better visibility of the core and better access to other experimental facilities. To maximize the beam flux, the port should be placed as close to the core as possible. Due to the presence of other experimental facilities and instrumentation, the available locations next to the core are limited. A possible solution

for the placement of the beam port is to use the FNIF. It has a flat top, which would work well for the placement of the beam tube. The neutron flux in the FNIF is fairly well characterized which would be beneficial in providing a baseline for calculation and reactor control [4]. The vertical beam port will be moveable to provide good access to the core when needed and will have the ability to use different apertures for different applications. The end of the beam port should be far enough below the surface of the pool to not need a biological shield other than the water existent in the pool. It should be a simple design to minimize cost and downtime. To accommodate different apertures the beam port will be composed of a two pieces. The aperture assembly will be separated from the beam port. This will provide the ability to use different apertures for different applications as needed. The most common apertures would be permanent fixtures, which would not be easy to modify. Some easily modifiable apertures could also be made to accommodate testing of new aperture designs or to create custom apertures, which would only be used for a short period before being changed. This aperture assembly would fit into the sample area of the FNIF and would have the same basic dimensions as the FNIF insert with the exception of the height. It would be designed to hold the bottom of the beam port in place on top of the FNIF. The beam port is put into place by placing it over the aperture on top of the FNIF. It must be secured at the top by mechanisms extending to the top of the pool secured to the framework of the control rod drives or the pool side.

3. The MCNP5 Model

Before manufacturing the beam port it is important to validate the design with calculations. The beam port design is modeled using MCNP5 [2] transport code. To speed up processing and improve the reliability of the results, the model was split into two parts. The first part of the model includes whole core and the FNIF surrounded by water as shown in Figure 1. Each fuel element was modeled individually as placed in its correct location. All the components of the FNIF were also modeled as accurately as possible based on original design drawings.

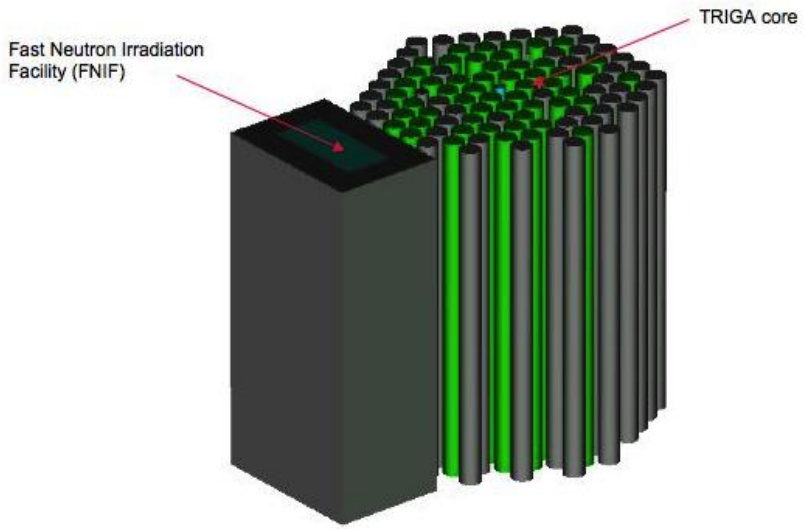

Figure 1. MCNP5 model of the UUTR FNIF and UUTR reactor core; FNIF contains lead shielding to reduce gamma components from the core; the maximum neutron flux at the center of FNIF is 3.0×10^{11} neutrons/cm^2·sec

The central part of the FNIF (the opening) was filled with air in our MCNP5 model. Neutron MCNP5 tallies for the core was set up in two locations. The first was a flux tally

for the central irradiator. The second was a current tally for neutrons crossing the top of the FNIF. A photon current tally across the top of the FNIF was also defined to characterize the photon spectrum. All the tallies in the models were divided into 200 energy bins to define a spectrum. The second part of the model relates to the port; the beam port assembly and the top opening of the FNIF is shown in Figure 2. Directly above the FNIF opening was approximately 10 cm of lead with 2.5 cm of graphite above that in contact with the lead. A square aperture (with the sides equal to 2.54 cm) was made of 0.25 mm thick gadolinium. The aperture was located approximately 5 inches above the FNIF opening in direct contact with the graphite. The beam port itself was modeled as being filled with the air. The bottom of the port was dimensionally the same as the FNIF top opening. The top was dimensionally the same as the sample box. There was approximately 350 cm from the aperture to the top of the beam port (the cassette loading area). The sample box had dimensions of approximately 53 cm long by 46 cm wide by 31 cm high. This sample box was divided by 9 circular sections such as area 1, area 2, area 3, etc., to calculate neutron and gamma fluxes on each area of the top of the sample box. The beam port was made of aluminum and its inside was filled with air. The results (photon and neutron energy and probability) from the second tally of the core model were used as the source terms for modeling the port. The source term was defined as a surface source distributed uniformly over the surface. The final tally was at the top of the cassette box. This was a current tally for neutrons and photons subdivided into nine segments as shown in Figure 3 to check the uniformity of the flux at the film cassette. Since MCNP5 only allows source definitions for a single particle type in the model, the beam port in the model had to be modeled once for the neutron source and once for the photon source. The tally results for each run then had to be combined into a final neutron tally and a final photon tally.

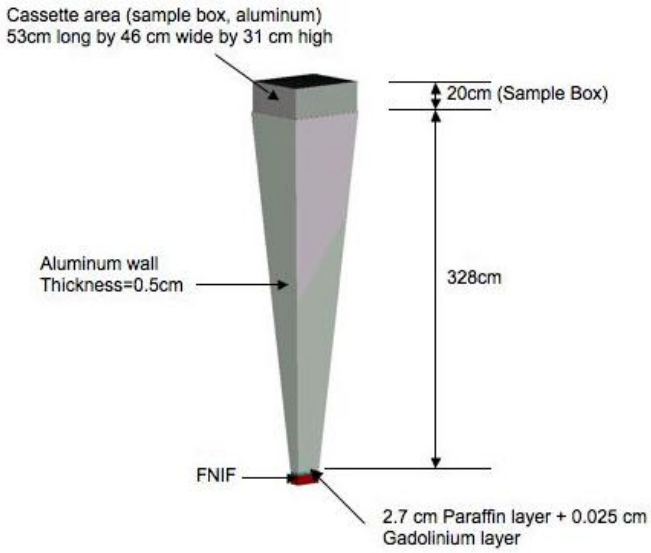

Figure 2. Vertical beam port; inside of the beam port is filled with air

4. Results

The first part of the model was run for a total of 1,101,770 particles. The relative error of the neutron current across the top opening of the FNIF was 0.0131. Results less than 0.10 are considered to be reliable. It should be noted that not all the energy bins had relative errors less than 0.10. However, all the bins below 8 MeV had relative errors below 0.10. The same tally for photons had a relative error of 0.0145. Since all the tallies

were eventually referenced back to the central irradiator neutron flux, the relative error of this tally is also of interest. The relative error of the central irradiator tally was 0.0132 with the majority of the lower energy bins having relative errors less than 0.10. The lowest energy bin to have a relative error larger than 0.10 is at 13.3 MeV.

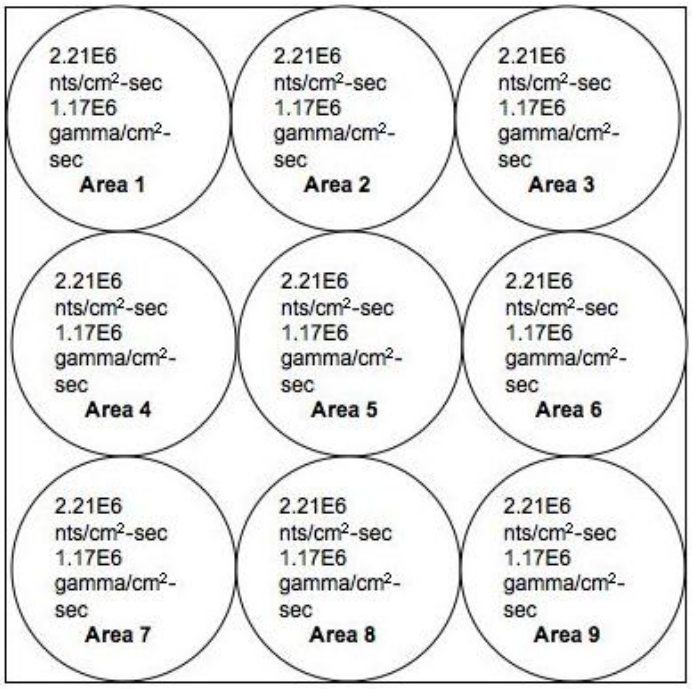

Figure 3. MCNP5 neutron and gamma fluxes on the top of the UUTR beam port

Normalizing the tallies to the central irradiator provided the ability to approximate the actual neutron and photon currents and flux across the top opening of the FNIF. The neutron flux was obtained to be 2.22 x 10^{10} neutrons/cm^2-sec at the top of the FNIF opening [8]. This is at the same level (height) as the top surface of the core. This measurement is credible because the neutron flux measurement halfway down (vertically) the FNIF results in 3.0 x 10^{11} neutrons/cm^2-sec, [4]. The neutron flux distribution is highest at the half way point (vertically) and tapers off going either direction (up or down). This axial neutron flux distribution in the FNIF is very similar to that of the central irradiator. The central irradiator has a maximum flux half way down (vertically) as well and presents a similar pattern of distribution. Using the neutron and photon current tallies' results across the FNIF as the source term in the second part of the model, neutron and photon tallies were obtained at the top of the experiment box (where the film cassette would be placed). It took 300 minutes using 207 million particles and the relative errors of all the photon tally segments were below 0.04. The second part of the model using the neutron source ran for a total of 10,570 minutes (7 days, 8 hours) resulting in 114 million particles being tracked. The relative errors of all the segment tallies for both neutron and photon were less than 0.02. As shown in Table 1 the average neutron current across all nine tally segments was 3.49 x 10^8 neutrons/sec or a flux of 2.21 x 10^6 neutrons/cm^2-sec. The standard deviation was 8.73% for the current or 1.22% for the flux. The average photon current was 1.86 x10^8 photons/sec or a flux of 1.18 x 10^6 photons/cm^2-sec. The standard deviation was 8.46% for the current or 2.09% for the flux. The neutron spectrum from MCNP5, over 70% of the neutrons were below 0.01 MeV. On the top of the beam port that is about 350 cm from the top of

the core, majority of the neutrons are thermal neutrons because there will be paraffin and graphite layers at the bottom of the beam port. For this modeling, neutron energy ranging from 0 to 20 MeV was divided by 200 equally spaced energy bins. The effect from fast neutrons on neutron radiography is negligible and it is important to set up more detailed tallies in the thermal neutron energy region in the future modeling [6]. For image detection, a thermal neutron to gamma ratio of 10^5 neutrons/cm^2-mR is required. In general, Gadolinium oxysulphide (GdOS) is used for the converter to lower the neutron flux for high image resolution. GdOS has a thermal neutron flux to gamma conversion ratio of $3x10^6$ neutrons/cm^2-mR and the minimum requirement of neutron flux for high resolution neutron radiography can be ~ $3.33x10^4$ neutrons/cm^2-sec [7].

Table 1. The average neutron and photon current across all nine tally segments

	Neutron			Photon		
	Average	Std Dev	% Change	Average	Std Dev	% Change
Flux	2.21E+06	2.69E+04	1.22%	1.18E+06	2.46E+04	2.09%
Current	3.49E+08	3.04E+07	8.73%	1.86E+08	1.57E+07	8.46%

5. Conclusions

According to the ASTM standards E78-02 (ASTM 2002) [3], if thermal neutron flux from a nuclear reactor is between 1E5 nts/cm^2-sec and 1E8 nts/cm^2-sec, it represents an excellent source for neutron radiography. High resolution radiography requires a total neutron flux of about 1E12 nts/cm^2-sec at the source and thermal neutron flux of 1E6 nts/cm^2-sec at an object [1]. From the calculations based on the MCNP5 for the University of Utah 100 kW TRIGA reactor, it is obvious that a vertical beam port is not only feasible, but also desirable. The major drawback to the design is the requirement to place samples in a water-tight box and lower them onto the top of the port. The advantages of a simple design with changeable apertures and no additional biological shielding requirement far outweigh the drawback for research purposes. If high volume production were desired, having to lower each sample through the water to the port would render this design virtually unusable. Though this design used the FNIF as a starting point, it is not dependent on using the FNIF. It would be a simple matter and may even be desirable to design a new base for the beam port. A new base for the beam port could be designed to improve the neutron beam quality instead of making with what is available. It should also be noted that in designing the aperture, fill materials (i.e. graphite, lead, water, etc.) for the opening of the FNIF should be investigated to possibly reflect more neutrons up the port. It would also be advantageous to create a complete accurate model of the core inclusive of all the facilities and verify the MCNP5 model. Any further modeling of the facility could always start with the verified benchmark model of the core resulting in increased confidence of the results.

6. References

1. Halmshaw, R. Industrial Radiography, 2nd edition, Sevenoaks, UK, Chapman & Hall, 1995.
2. X-5 Monte Carlo Team, MCNP5 manual, Los Alamos national laboratories, Oak Ridge, Tennessee, 2003.
3. Annual Book of ASTM, Standard particles for thermal neutron radiography of materials, Designation E748-02, ASTM 2002.
4. John Bennion, Characterization and Qualification of a Quasi-Fission Neutron Irradiation Environment for Neutron Hardness Assurance Testing of Electronic Devices and Other Materials Damage Investigations, Ph.D. Dissertation, The University of Utah, 1996.
5. Safety Analysis Report for the University of Utah 100 kW TRIGA Reactor, the University of Utah, 1985.

6. Domanus, J. C., Practical neutron Radiography, Norwell, Massachusetts, D. Rediell Publishing, 1992.
7. Peter, V. D. H., Rottger, H., Neutron radiography Handbook, Hingham, Massachusetts, D. Reidel Publishing, 1981.
8. Thompson, R. J., Investigation of a flux trap for a TRIGA reactor, MS Thesis, the University of Utah, 1982.

MONTE CALRLO MODELLING OF VOID COEFFICIENT OF REACTIVITY EXPERIMENT

R. KHAN, M. VILLA, H. BÖCK
Vienna University of Technology
Atominstitute
Stadionallee 2,
A-1020, Vienna, Austria

ABSTRACT

The Atominstitute (ATI) of the Vienna University of Technology utilizes a TRIGA Mark II research reactor for last fourty eight years at a nominal reactor power of 250 kW (thermal). It has a completely mixed core and employing three different types of fuels i.e. aluminium clad fuel with 20% enrichment, stainless steel (SS) clad fuel with 20% enrichment and SS clad FLIP fuel with 70% enrichment. The current core loading is 83 fuel elements. The reactor core is equipped with many irradiation facilities inside the core to irradiate samples at different flux levels. These irradiation facilities include the Central Channel (CC which is used to irradiate samples at maximum flux. This paper presents the calculations and measurements of the void coefficient of reactivity in CC. For this purpose, a cylindrical void of 66.47 cm^3 was inserted into the CC and moved from bottom to top of the core along the axial length of the channel in steps of 5 cm. For each step, the effect of void sample on the core reactivity was measured by the regulating control rod position. This experiment was performed at 10W in automatic mode of operation.
Monte Carlo neutronics simulating code, equipped with the cross sections library JEFF 3.1, was employed to perform these calculations. For each 5 cm step in the central irradiation channel, a separate model was executed. To see the influence of the control rods, the MCNP calculations were performed. In theses calculations, the control rods were set to the reactor operating conditions. Both the simulated and measured results were compared. Fairly good agreement was observed between calculations and experimental results.

1. Introduction

The Atominstitute (ATI) of Vienna University of Technology utilizes the TRIGA Mark II research reactor for its research, training and educational interests for last 48 years. The reactor operates at an average power level of 250kW and is equipped with many irradiation facilities inside and outside the reactor core. Inside the core, there are many irradiation channels including central thimble CC which is used for high flux irradiation. Starting with 57 Fuel Elements (FE(s)) of same type in 1962, the current core has 83 FE(s) of three different types. Out of 83 FE(s), 54 are 102-type (Aluminium-clad, 20% enriched), 20 are 104-type (Stainless Steel-clad, 20% enriched) and 9 are FLIP (SS-clad, 70% enriched) FE(s). These FE(s) are cylindrical in geometry and are arranged into 5 concentric circles (rings) in an annular lattice [1]. The schematic diagram of TRIGA FE is shown in Figure 1[2].

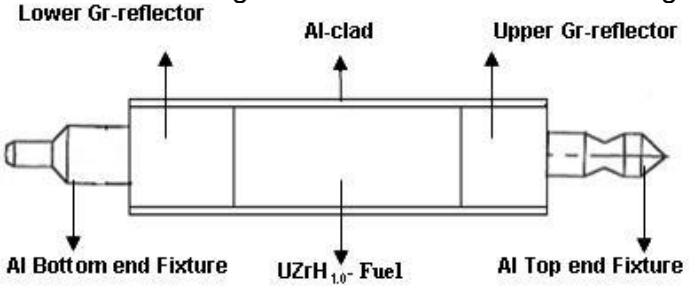

Fig 1. Schematic diagram of TRIGA Mark II reactor fuel element [2].

The reactor utilizes zirconium hydride fuel which is a homogeneous mixture of uranium (U) and zirconium hydride (ZrH). The ZrH is used as main moderator. About 80% of the neutron

moderation occurs inside the fuel. Since the moderator has the special property of moderating less efficiently at high temperatures, the TRIGA reactor can produce a pulse of 250 MW for roughly 40 milliseconds [1].

The operational safety of the reactor needs the information of reactivity effects on the core caused by small disturbances. To investigate the void effect on the core reactivity, this work focuses on the calculation of the void coefficient of reactivity and its experimental confirmation in the central irradiation channel CC. The current core map including in-core irradiation facilities is shown in Figure 2.

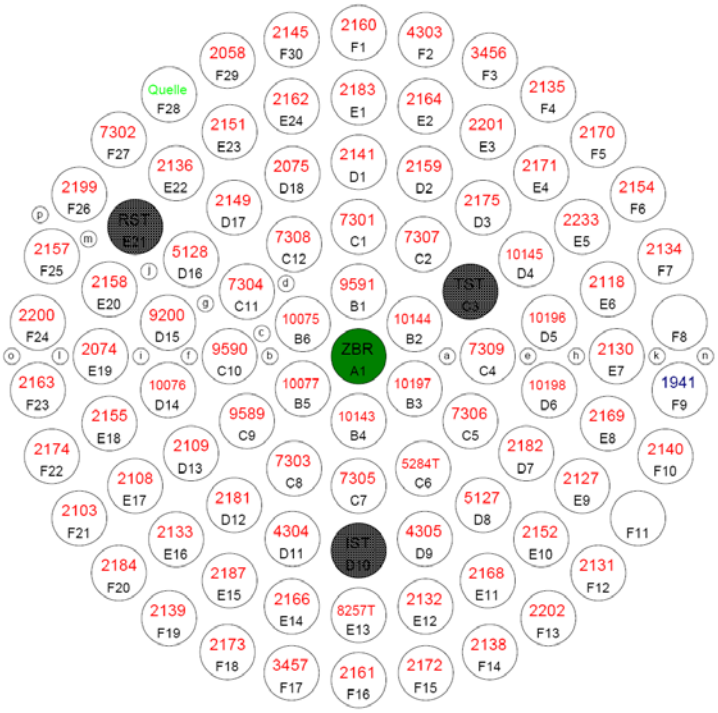

Fig 2. The current core map of the TRIGA Mark II research reactor.

1.1 Void Coefficient of Reactivity

The dominant reactivity effect in water moderated reactors arises from the changes in moderator density, due to either thermal expansion or void formation. The principal effect is usually the loss of moderation that accompanies a decrease in moderator density and causes corresponding increase in resonances [5]. In contrast with water moderated reactors, about 80% of the moderation occurs inside the fuel of TRIGA reactors. Therefore void effects on core reactivity of TRIGA reactor is studied in the paper.

Core reactivity, for given value of K_{eff} is determined by the relation [3]

$$\rho = \frac{K_{eff} - 1}{K_{eff}} \qquad (1)$$

Generally the reactivity coefficient is defined as the change in reactivity for a given change in parameter [4]. Mathematically written as

$$\gamma_{\xi} = \frac{\Delta \rho}{\Delta \xi} \qquad (2)$$

Here ξ is reactor parameter that affects reactivity and $\Delta\rho$ is the corresponding change in reactivity. If the ξ represent void (or V_D) then γ_{ξ} defines the void coefficient of reactivity [3]. The actual value varies from reactor to reactor. In this work, the effect of a void (in CC) on the TRIGA core reactivity is studied.

2. Measurements: Void Coefficient Experiment

This experiment was performed at ATI reactor at 10W reactor power. The reactor control was set to automatic mode and the regulating rod was selected as the only reactivity controlling variable for this experiment. The regulating control rod was selected because it is capable of achieving a finer control of the core as compared to the other two control rods. The 66.47 cm^3 void sample in an airtight cylindrical polyethylene bottle of length 10.8 and a radius of 1.4 cm was prepared at ATI. This sample holder was attached to a string and inserted into CC. The sample was first placed at the bottom of the core and then raised in 5 cm steps along the axial length of CC. Each step of the sample was followed by a period to stabilize the reactor state before the regulating control rod position was recorded. Using the regulating control rod calibration curve, the reactivity for each length of regulation control rod was recorded and given in Table 1.

Void sample position	Regulating CR position	Reactivity of void (cents)
0	207	
5	220	-2.947
10	218	-2.471
15	218	-2.471
20	208	-0.137
25	195	2.884
30	187	4.739
35	192	3.582
40	201	1.516
45	213	-1.294
50	210	-0.633
55	206	0.276
60	204	0.772
65	204	0.772

Table 1: Measurements of void coefficient of reactivity

3. Calculations: Void Coefficient of the Reactivity

To calculate the void effect on reactor the core, a detailed three dimensional computational model of the TRIGA Mark II reactor was developed using the Monte Carlo neutronics behaviour simulating code MCNP5 [5]. Because of lack of Samarium cross sections in ENDF-VI, the computer program employs JEFF3.1 as cross section library in these computations. This model includes reactor core components, surrounding graphite reflector, four beam tubes and the thermal column as shown in Figure 3. The reactor core components are comprised of 83 burned FE(s) of three different types, three control rods, one source element (in F28 position), two pneumatic systems (in F08 and F11 positions) and a central irradiation channel CC. This MCNP model is based on standard experiments performed on TRIGA Mark II reactor of ATI. These experiments include the criticality experiment, reactivity distribution experiment and radial and axial flux distribution experiment on the burned reactor core.

The developed MCNP model, incorporating the burned fuel composition, was modified to calculate the void coefficient in the central channel. The experimental procedures, described in section 3, were applied to the MCNP model to calculate the void coefficient of reactivity in the CC. The model was modified and executed for each step length separately along the axial length of the CC. The top view of the MCNP model is given in Figure 3. The vertical (YZ) view of the model shows the modelling of the sample, holding the void in vertical channel CC in Figure 4.

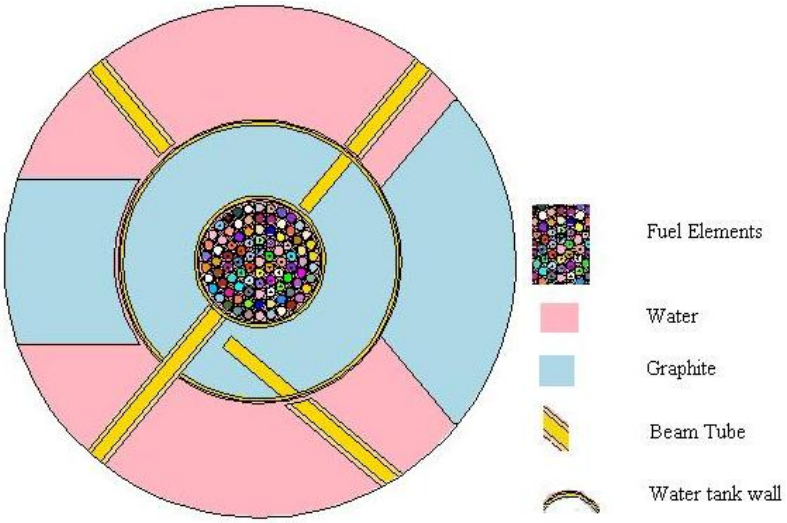

Fig 3. Top (XY) view of the MCNP model of TRIGA Mark II reactor

These calculations were carried out with total number of 200 cycles of iteration on a source size of 500 000 particles per cycles. To decrease the statistical error estimates, the first 50 cycles were skipped. For each execution, the void sample was moved 5cm up in axial direction. From the output, K_{eff} for each run was obtained to calculate the corresponding reactivity effect in dollars the using effective delayed neutron fraction β= 0.0073. The calculated results are compared with experimental observations in section 4.

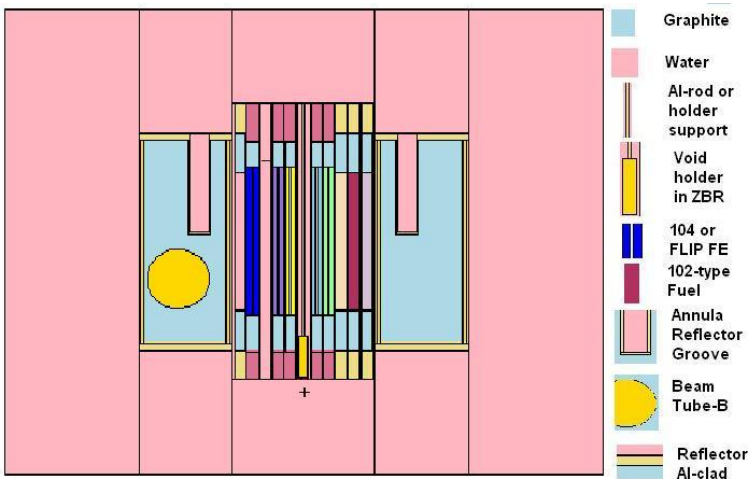

Fig 4. Vertical (YZ) view of the MCNP model of void coefficient

To eliminate the control rod effect on voids, second series of calculations were performed keeping all three CR in fully withdrawn positions. In these calculations, a source size of 5000 particles, 200 neutron cycles skipping first 50 cycles were applied to the model. These results are discussed in section 4.

4. Results and Discussions

Figure 5 shows the comparison between calculations and measurements. From these results, it is observed that reactivity effects on the TRIGA reactor due to void in the central channel is not very significant. From Table 1, it ranges from -0.044 to 0.073 cents per cubic centimetres. It is also observed that, in contrast to other water moderated reactors, void may introduce a positive reactivity in TRIGA reactors. It is due to the unique fuel properties. Figure 5 shows that MCNP predictions follow the experimental results. The fact is that a cylindrical void of about 66.47 cm^3 in CC, introduces a negative reactivity when placed at the top and bottom part of the reactor core and it add a positive reactivity when moved through

the active length of the core. This may be due to the fact that the much lower neutron scattering cross section of the air provides an easy escape route to neutrons out of the core at both ends of the core. On one side, in the active part of the core, this void replaces the moderator and reduces the moderation resulting into the introduction of negative reactivity in the core. While on the other side, due to the low absorption cross section of void than water (moderator), it reduces the neutron absorption and introduces positive reactivity. It was shown theoretically and experimentally that the overall effect of this void in the CC is positive after compensating the negative reactivity due to decrease in moderation.

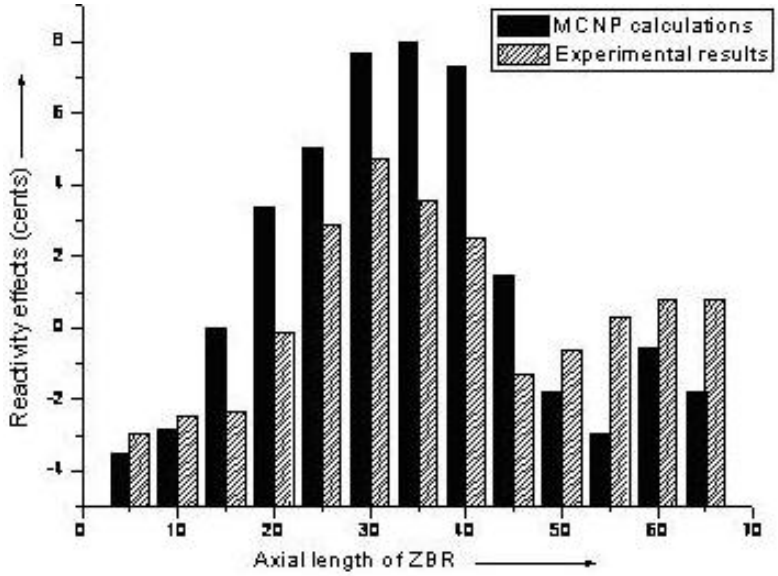

Fig 5: Theoretical and experimental comparison of void coefficient of reactivity

5. Conclusion

The MCNP model was developed for the neutronics analysis of the TRIGA Mark II reactor core. The developed model was modified to calculate the void coefficient of the reactivity in the central channel of the reactor. The calculations were verified experimentally. In contrast to other water-moderated reactors, the effect of void compensates the negative reactivity introduced due to decrease in moderation and overall introduces a positive reactivity in the CC. At the top and bottom ends of the core, the void effect is negative due to neutron leakage out of the core. Generally, the MCNP predictions follow the experimental observation along the length of central irradiation channel.

6. References

1. General Atomic (GA), March 1964. TRIGA Mark II Reactor General Specifications and Description. General Atomic Company, U.S.A.
2. R. Khan, S. Karimzadeh, H. Boeck, 2009. TRIGA fuel Burn up calculations supported by gamma scanning. RRFM 2009, IAEA, Vienna, Austria.
3. R. Khan, T. Hamid, 2006, “Feedback Reactivity Coefficients and their Coupling”, NED 46711-6.
4. Karl O. Ott and Robert J. Neuhold, 1985, “Introductory Nuclear Dynamics”, American Nuclear Society, La Grange Park, Illinois, USA.
5. Monte Carlo Team, “MCNP – A General Monte Carlo N-Particle Transport Code, Version 5”, LA-UR-03-1987, Los Alamos National Laboratory, April 24, 2003.
6. James J. Duderstadt and Louis J. Hamilton, 1976, “Nuclear Reactor Analysis”, John Wiley and Sons, New York

European Nuclear Society

Rue Belliard 65, 1040 Brussels, Belgium
Telephone +32 2 505 30 54, Fax + 32 2 502 39 02
rrfm2010@euronuclear.org - www.euronuclear.org